Gel polymer electrolytes design for Na-ion batteries

*Jun Pan, Nana Wang, and Hong Jin Fan**

J. Pan, Prof. H. J. Fan

School of Physical and Mathematical Sciences, Nanyang Technological University, Singapore 637371, Singapore

Email: fanhj@ntu.edu.sg

Dr. N. N. Wang

Institute for Superconducting and Electronic Materials, University of Wollongong, Innovation Campus, Squires Way, Wollongong, New South Wales 2500, Australia

Keywords

Gel polymer electrolytes, quasi-solid-state electrolytes, intermolecular interactions, interfacial properties, Na-ion batteries

ABSTRACT

Na-ion battery has the potential to be one of the best types of next-generation energy storage devices by virtue of their cost and sustainability advantages. With the demand for high safety, the replacemlent of traditional organic electrolytes with polymer electrolytes can avoid electrolyte leakage and thermal instability. Polymer electrolytes, however, suffer from low ionic conductivity and large interfacial impedance. Gel polymer electrolytes (GPEs) represent an excellent balance that combines the advantages of high ionic conductivity, low interfacial impedance, high thermal stability, and flexibility. This short review summarizes the recent progress on gel polymer Na-ion batteries, focusing on different preparation approaches and the resultant physical and electrochemical properties. Reasons for the differences in ionic conductivity, mechanical properties, interfacial properties, and thermal stability are discussed at the molecular level. This Review may offer a deep understanding of sodium-ion GPEs and may guide the design of intermolecular interactions for high-performance gel polymer Na-ion batteries.

1. Introduction

As a typical secondary energy storage battery, lithium-ion batteries (LIBs) with high energy density and low self-discharge are widely used in various fields of life.[1,2] Na-ion batteries (NIBs) have similar working principle to LIBs, and their low price and abundant reserves are expected to enable them to complement or replace LIBs.[3,4] The traditional organic electrolytes, however, are unable to meet the needs for high safety and a wide operating temperature range due to the risk of leakage and low thermal stability. Therefore, it is urgent to explore new-type of electrolytes.[5,6]

Although replacing the traditional liquid electrolyte with an all-solid-state electrolyte is the ultimate method to solve the above problems,[7-11] at present, it is difficult to directly meet the current needs. Inorganic solid electrolytes (such as β-alumina, sodium superionic conductor and sulfide-based solid-state electrolytes) suffer from the difficulty in mass production, the high brittleness and poor interfacial compatibility/stability with electrodes.[12-16] In contrast, polymer solid-state electrolytes (including polyethylene oxide, polyacrylonitrile, polymethylmethacrylate and polyvinylidene fluoride) possess flexibility and improved interfaces, but the low ionic conductivity limits the applications.[17-74] Therefore, the gel polymer electrolyte (GPE) with combined advantages of liquid electrolytes and polymer electrolytes to achieve high ionic conductivity and good interfacial contact have drawn great attention in recent years. Besides, the addition of inorganic electrolytes or fillers can further improve their thermal stability and mechanical properties.[75-78] There has been no review articles on the synthesis of Na-ion GPEs and deep insights to their physical and electrochemical properties.

This short Review focuses on the recent advances in sodium ion GPEs (**Figure 1**). Firstly, typical synthesis approaches are categorized and summarized, including immersion, solution casting, and *in-situ* polymerization. Specifically, for the immersion approach, polymer membranes prepared by the solution method, phase separation, or electrospinning are soaked into

the chosen organic electrolyte, during which, oxides, ionic conductors, or glass fiber can be added to further enhance the performance. The solution casting approach involves adding plasticizers or ionic liquids when dissolving the sodium-salt-polymer to prepare a gel electrolyte with strong interaction. In the *in-situ* polymerization approach, separator-supported or self-supported GPE membranes with adjustable interfaces can be prepared by means of light, heat, initiators, or self-polymerization. After elaborating the synthesis methods, the different physical/electrochemical properties of GPEs from various synthesis methods are analyzed from the molecular level. Finally, we propose our perspective on future research directions. With the development of Na-ion GPE designs and the suitability of NIBs for supplementing the dominant Li-ion batteries, more attentions are being paid to gel polymer NIBs from the aspect of safety concerns. We hope that this review will be helpful for the development of Na-ion GPEs and gel polymer NIBs.

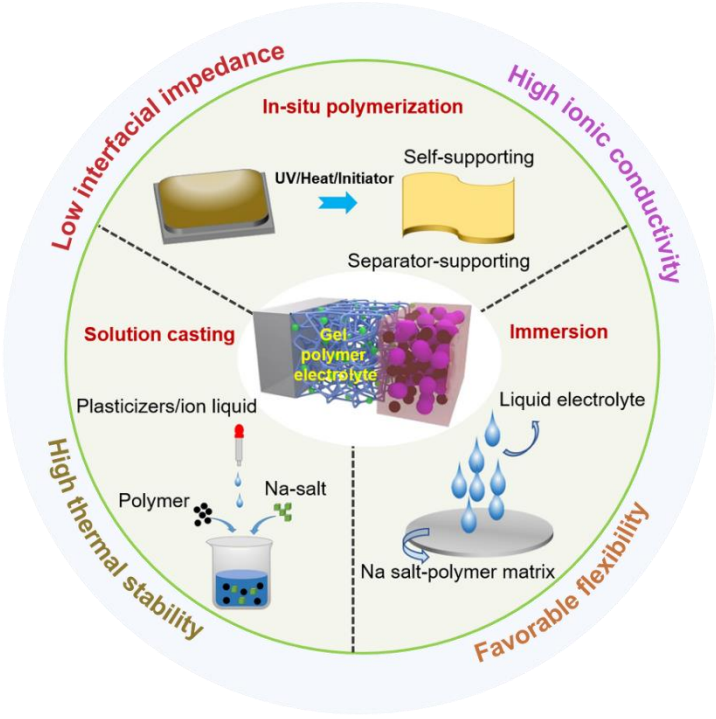

Figure 1. Typical synthesis approaches to Na-ion gel polymer electrolytes (GPEs) and their properties.

2. GPE by immersion approach

The immersion approach is a simple method to prepare gel electrolytes, that is, they are mainly prepared via swelling dry polymer membranes in organic liquid electrolytes. Specifically, a suitable polymer substrate is selected, and polymer membranes of different sizes, thicknesses and porosity are prepared by solution, phase separation, or electrospinning methods.[79,80] Next, the membranes are soaked in the desired organic electrolyte for a period of time to swell the polymer and squeeze out the excess liquid to obtain a flexible gel electrolyte membrane with high ionic conductivity gel electrolyte membrane.[81,82] Inorganic fillers can be added when preparing the polymer membrane to further promote the mechanical strength and thermal stability of the membrane.[83,84] This is a promising method for large-scale fabrication of gel electrolyte membranes.

2.1 Polymer membrane soaked in electrolyte

The properties of the polymer precursor membrane are decisive to the electrochemical performance, so the preparation method for the polymer membrane is very critical. The current common synthesis methods include solution, phase separation, and electrospinning methods. Their specific properties are described below with specific examples.

Su et al. synthesized a Na-ion-conducting GPE based on poly(vinylidenefluoride-co-hexafluoropropylene) (PVDF-HFP) membrane that was soaked in 1 mol L^{-1} $NaClO_4$ with fluorinated ethylene carbonate (FEC) and propylene carbonate (PC) solvents for use as both the electrolyte and the separator.[85] Abundant pores are advantageous for absorbing and holding the liquid electrolyte, and a high ionic conductivity (0.42 mS cm^{-1}) was obtained at room temperature. The GPE exhibited the better thermal stability compared with commercial separator containing the same amount of electrolyte. Moreover, the evaporation rate of the organic electrolyte in this GPE was slower, indicating much enhanced retainability of the liquid electrolyte.

Based on this GPE design, hard cotton//$Na_3V_2(PO_4)_2O_2F$ (NVPOF) cloth full cell exhibits a high-capacity retention of 90% even after 500 cycles at 1 C (**Figure 2**a). In order to further increase the sodium ion transference number (t_{Na^+}), Cui et al. reported a single ion-conducting GPE membrane containing polymeric sodium tartaric acid borate (PSTB) and poly(vinylene carbonate) (PVCA) soaked in ethylene carbonate (EC)/diethyl carbonate (DEC) organic solvents (PSP_{10}-GPE), which exhibited high t_{Na^+} and excellent interfacial compatibility.[86] The high t_{Na^+} (0.88) was efficacious in alleviating the concentration polarization and impeding the formation of Na dendrites due to the moving anions. Moreover, Feng et al. increased the t_{Na^+} to 0.91 through combining a new sodium-poly(tartaric acid)-borate salt (NaPTAB) with PVDF-HFP swollen with PC solvent (NaPTAB-SGPE) (Figure 2b and 2c).[87] The reason is that the anions in NaPTAB are fixed to the polymer chains of PVDF-HFP, leading to the interaction of F atoms with the H atoms of $-CH_2$ groups, which reduces the polarity of $-CF_2$ and weakens the interaction between the polymer chain and Na^+ ions, thereby accelerating the migration of Na^+ ions. In addition, PC acts as a plasticizer distributed between macromolecular chains to reduce intermolecular forces.

Ionic conduction in GPEs can take place through the liquid electrolyte trapped in the pores of the polymer matrix and the swelling of the amorphous domains by the liquid electrolyte. Therefore, it is particularly important to create pores in the GPEs. Phase separation is an effective method for creating pores by using water as the non-solvent and pore producer.[88] Park et al. prepared a configurable GPE with a controllable pore structure via a simple nonsolvent-induced phase separation method that allowed for the absorption of more liquid electrolyte (Figure 2d and 2e).[89] The obtained PVDF-HFP coated glass-fiber (GF) membrane exhibited a uniform micropore pathways for sodium ion transfer and a porous outer PVDF-HFP layer acting as a strong electrolyte absorber that improved the interfacial adhesion between the GPE and the electrodes.

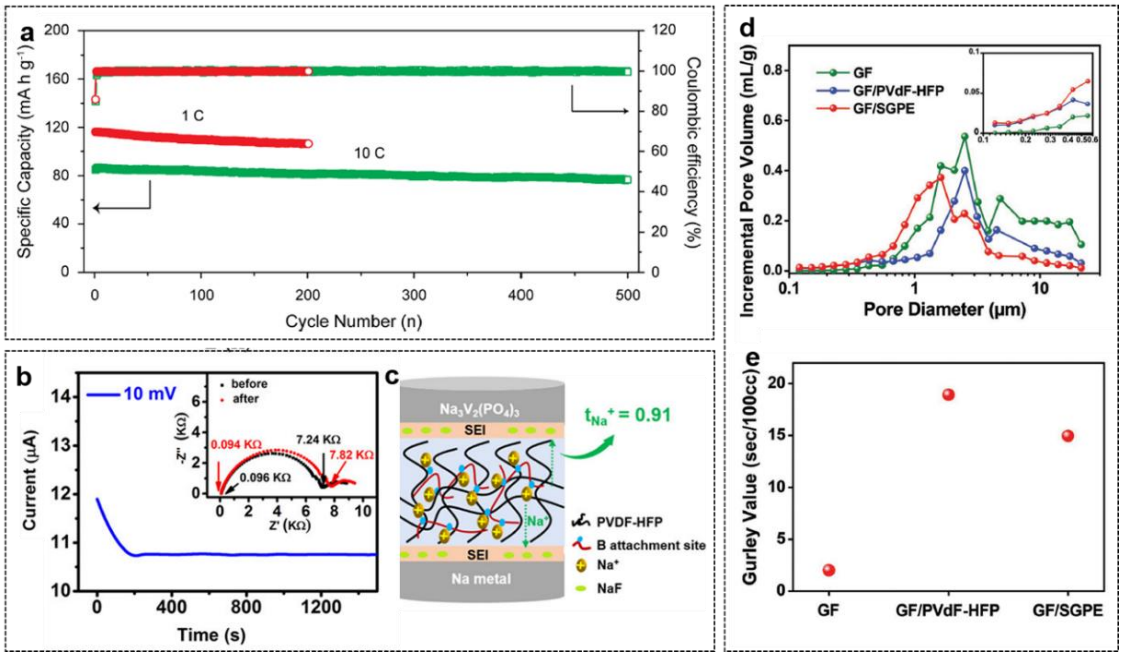

Figure 2. GPE and gel polymer prepared by immersion electrolyte approaches. (a) Cycling stabilities of hard cotton//NVPOF full cells at two current densities. Reproduced with permission.[85] Copyright 2018, American Chemical Society. (b) DC polarization of NaPTAB-SGPE symmetrical cell at 60 °C (inset: electrochemical impedance spectroscopy (EIS) spectra of the cell). (c) Schematic of a $Na_3V_2(PO_4)_3$//NaPTAB-SGPE//Na full battery. Reproduced with permission.[87] Copyright 2020, American Chemical Society. (d) Porosimeter data and (e) Gurley value of the prepared separators. Reproduced with permission.[89] Copyright 2017, Wiley-VCH.

Compared with the phase separation method, electrospinning is an extraordinary technique to prepare large-area polymer fibrous membranes that have pore sizes ranging from several nanometers to a few micrometers and an interconnected network structure.[90] The abundant pore structure and large specific surface area can lead to more electrolyte uptake, leading to high ionic conductivity for the obtained GPE. Venimadhav et al. reported an electrospun PVDF-HFP membrane with a high ionic conductivity (1.13 mS cm^{-1}) that was activated by submerging it in an electrolyte solution of 1M $NaClO_4$ in EC/DEC.[91] The gelled membrane showed good Coulombic efficiency retention of 97% when evaluated in a $NaNi_{0.5}Mn_{0.5}O_2$//Na cell at a current density of 0.1 C after 50 cycles, which is attributed to its high porosity, bead-free morphology, and uniform fiber distribution. The electrolyte membrane prepared by the above method had good ionic conductivity, although its mechanical strength and thermal

stability need to be further improved towards application.

2.2 Ceramic-polymer membrane soaked in electrolyte

In polymer sodium-ion batteries, the addition of ceramic fillers is a direct way to improve the ionic conductivity. The specific reasons are as follows: 1) The crystallinity of the polymer is reduced by adding the ceramic fillers, which promote structural modification of the polymer chains and Na^+ conducting pathways at the filler surface. 2) Dissociation of sodium salts is facilitated by the formation of an "ionic ceramic complex" due to Lewis acid-base interactions. The above conduction mechanism, however, is not the rate-determining step in a GPE. In the case of a GPE, the main purpose of adding ceramic fillers is to improve its mechanical strength and thermal stability. In order to further improve the ionic conductivity and interface compatibility of GPEs, it is advisable to create pores or form three dimensional (3D) structures to increase the absorption of liquid electrolyte.[92-95] Two examples are provided as follows:

A 3D porous GPE constructed from PVDF-HFP cross-linked with Al_2O_3 nanoparticles (PHP5A) has been designed, which showed with dramatically enhanced ionic conductivity up to ~1.3 mS cm^{-1} after soaking in electrolyte (**Figure 3**a and 3b).[96] The intermolecular hydrogen bonding between the -OH functional groups on the surfaces of the Al_2O_3 nanoparticles and the -C-F- functional groups in PVDF-HFP made the PVDF-HFP skeleton more mechanically robust. Moreover, the weak interactions between PHP5A and the carbonyl/ester groups promoted the formation of uniform GPEs. In the meantime, Ramaprabhu et al. used phosphorus containing hydroxyapatite as an inorganic filler incorporated in PVDF-HFP blended with poly(butylmethacrylate) (HAP).[97] The thus-formed HAP-GPE membrane was thermally stable up to 500 K because of the uniform distribution of hydroxyapatite. This HAP-GPE membrane also showed good mechanical stability, since the presence of functional groups in hydroxyapatite helped to form a composite structure within the polymer network.

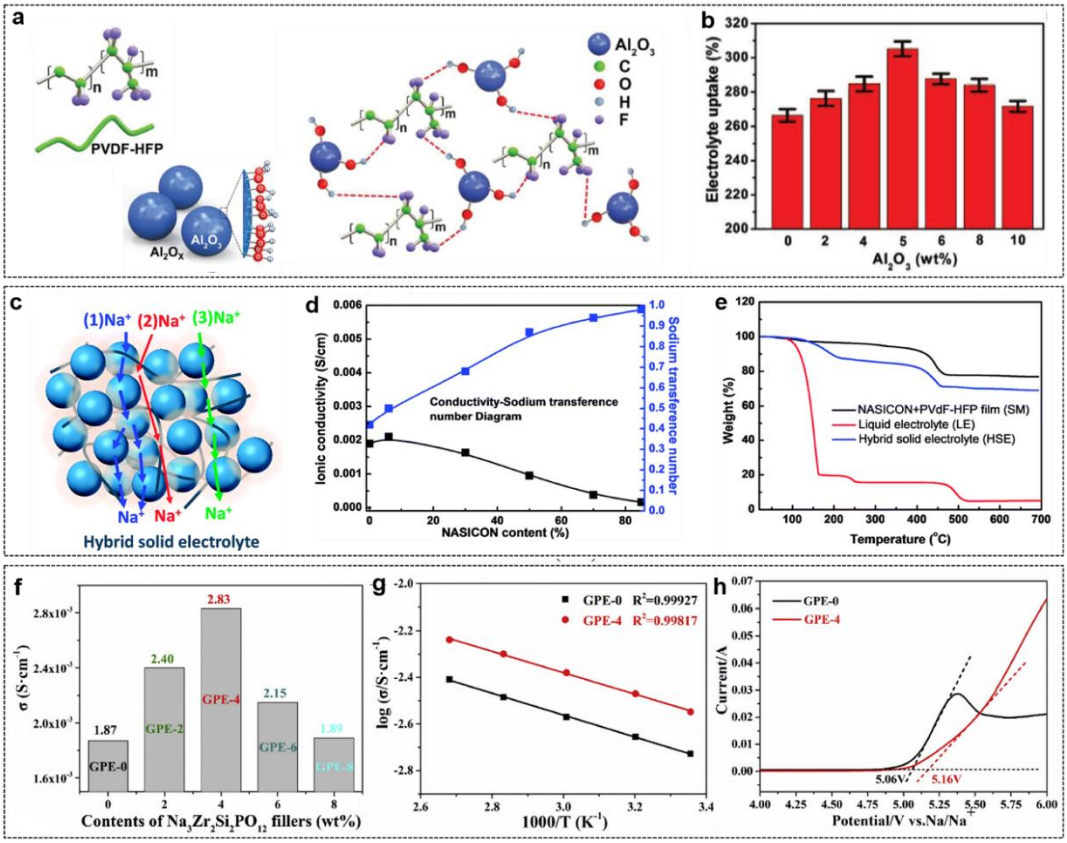

Figure 3. Physicochemical properties of GPE-containing ceramics. (a) Schematic of the quasi-solid-state polymer formed from PVDF-HFP and Al_2O_3 nanoparticles through Lewis acid-base intermolecular bonding. (b) Electrolyte uptake analysis of GPE as a function of A_2O_3 content. Reproduced with permission.[96] Copyright 2020, Wiley-VCH. (c) Model representation of a composite hybrid solid electrolyte (HSE) with sodium ion conduction paths. (d) Plot of the conductivity and Na migration number contributed by ion hopping and plasticizer ion transport. (e) Thermogravimetric analysis (TGA) results on a composite solid membrane, ether-based liquid electrolyte, and HSE. Reproduced with permission.[98] Copyright 2015, The Royal Society of Chemistry. (f) Ionic conductivity of the resulting GPEs films at room temperature, modified with variable filler contents. (g) Ionic conductivity versus temperature. (h) Linear-sweep voltammetry curves obtained for GPE-0 and GPE-4 films. Reproduced with permission.[99] Copyright 2021, Elsevier.

Unlike ceramic fillers, Na ionic conductor fillers can contribute to the Na^+ migration. Kim et al. reported a $Na_3Zr_2Si_2PO_{12}$-PVDF-HFP composite hybrid solid electrolyte (HSE) soaking in a solution of 1 M $NaCF_3SO_3$/tetraethylene glycol dimethyl ether (TEGDME) with fast ionic conductivity, a large Na^+ migration number, and high thermal stability.[98] The fast charge transfer and rapid Na^+ diffusion was ascribed to the formation of an ionically conducting liquid

medium on the polymer and ceramic surfaces via sodium superionic conductor (NASICON) Na-ion hopping (Figure 3c). The fast t_{Na^+} (0.92) may be due to the capture of anions by $Na_3Zr_2Si_2PO_{12}$, which promotes the transfer of Na^+ ions (Figure 3d). The high thermal stability was attributed to the stronger liquid molecular bonds in the liquid medium, while the HSE helps to absorb and preserve the liquid electrolyte within the pores, reducing the tendency towards rapid evaporation (Figure 3e). Recently, Wang et al. used $Na_3Zr_2Si_2PO_{12}$ in a PVDF-HFP/polymethylmethacrylate (PMMA)/thermoplastic polyurethane (TPU) matrix to make holes to accelerate the electrolyte uptake.[99] The enhancement of ionic conductivity by $Na_3Zr_2Si_2PO_{12}$ filler is mainly because it raises the membrane porosity, which improves the absorption rate of liquid electrolyte (Figure 3f and 3g). Then, the added $Na_3Zr_2Si_2PO_{12}$ filler itself is an ionic conductor, so it can rapidly conduct Na ions at the interface between the polymer and the conductive filler, which is superior to the performance of non ionic-conductor fillers. Moreover, it has a wider electrochemical reaction window of 5.16 V (GPE-4) than that without fillers (GPE-0), which implies that the addition of $Na_3Zr_2Si_2PO_{12}$ filler can improve the electrochemical stability of GPEs (Figure 3h). The obtained $Na_3V_2(PO_4)_3$ (NVP)//Na cell delivered a high capacity of 83.9 mAh g^{-1} at 5 C, owing to the enhancement of sodium ionic conductivity and interfacial stability due to the added $Na_3Zr_2Si_2PO_{12}$.

3. GPE by solution casting approach

The solution casting approach consists of mixing sodium salt, polymer, plasticizer, and filler together, heating and stirring to dissolve the components, and casting and drying to obtain the GPE. The plasticizers can be selected from solvents such as EC, DEC, PC, fluoroethylene carbonate (FEC), and ether, or it can be an ionic liquid with a high melting point and non-flammability. Compared with the immersion method, the gel membrane prepared by the solution casting method has stronger intermolecular interactions, that is, the plasticizer is bonded to the

polymer chain through the interaction of dehalogenation, nucleophilic substitution, and other reactions that occur during mixing.[100-107] Therefore, the resultant owned GPE membrane has higher thermal stability.

3.1 Plasticizer solvent addition

The plasticizer and polymer should be carefully selected to achieve a unification of ionic conductivity, interfacial contact, mechanical strength, and thermal stability through the interaction. For example, Chen and co-workers prepared a high conductive GPE (PVC, 7.5% + PVDF, 17.5% + $NaClO_4$, 8% + PC, 67%) using a solvent casting technique. It was demonstrated that the addition of PVC can cut down the long-range order of PVDF, resulting in the lower crystallinity, and thus favoring fast Na^+ ion movement in the polymer network. In addition, differential scanning calorimetry (DSC) curves showed a single peak in the range of 289-310 °C, indicating the good miscibility of the polymers in the blend. The glass transition temperature (T_g) values of the blended polymer membranes were higher than those of both mother polymers, which indicates a strong interaction between the PVC and PVDF. In another example, fast Na^+ ion transport channel was constructed by doping NaI, EC and dimethyl formamide (DMF) in high mechanical strength polyacrylonitrile (PAN) through solution casting.[109] The enhanced conductivity was ascribed to the weak electrostatic interactions between Na^+ and C=O groups of the plasticizers and the C≡N groups of PAN. Furthermore, PAN is also a flame-retardant polymer with low thermal resistance. The PAN-based GPE formed with $NaClO_4$, EC, and PC features high ionic conductivity of 4.5 mS cm^{-1} and showed outstanding stability (no noticeable weight loss) at temperatures up to 100 °C. [110]

The ionic conductivity, mechanical strength, and thermal stability of GPE can be further improved by adding ceramic fillers. For example, dispersing SiO_2 into a PMMA-$NaClO_4$-EC-PC GPE improves the ionic conductivity, thermal stability, and ion mobility number.[111] The

improved performance can be attributed to the following aspects. First, ion-filler-polymer interactions can enhance the ionic transport of the GPE films. Second, the SiO_2:ClO_4^- species form space-charge regions and induce a local electric field, which is beneficial for dissociating the Na salts and enhancing the number of free anions. Third, the added SiO_2 can improve the thermal stability of GPE (from -80 to 140 ℃). In the following research, TiO_2, Al_2O_3, ZrO_2, and $BaTiO_3$ were also used in GPEs to improve battery performance, and Al_2O_3 is most outstanding among them. For example, a thermally stable GPE film with high ionic conductivity and good interfacial contact was prepared through the introduction of Al_2O_3 into a polyethylene oxide (PEO)-$NaNO_3$-EC-PC matrix by the solution casting approach.[112] The addition of Al_2O_3 functionalized the GPE surface by forming O-OH groups on the surfaces of the grains, which led to the formation of hydrogen bonding with the migrating ionic species. Therefore, the obtained GPE had a more uniform dispersion of pores, which helps to reduce the interfacial resistance of the electrodes. More importantly, the GPE films retained good thermal stability up to 400 °C, as proved by the thermal studies.

3.2 Ionic liquid (IL) addition

Compared with traditional solvents, ionic liquids composed entirely of ions possess valuable properties such as low flammability, and high thermal and chemical stability. The main advantages are as follows: 1) The absence of molecules can eliminate interfacial side reactions and improve the Coulombic efficiency. 2) The tunable solvent can inhibit the corrosion of aluminum current collectors and the dissolution of active electrode materials. 3) The ILs are beneficial for reducing the charge transfer resistance at the electrodes.[113-126]

Using the solution casting method, Singh et al. reported a GPE composed of sodium bis(trifluoromethylsulfonyl)imide (NaTFSI), PEO, and 1-butyl-3-methylimidazolium bis(trifluoromethylsulfonyl)imide (BMIMTFSI) ionic liquid (10-40 wt.%), which functioned as the

plasticizer.[127] As increased amounts of ILs were incorporated in the GPE, the T_g and the melting temperature (T_m) both shifted to lower temperature because of the plasticization effect, indicating that the elasticity and free volume of the polymer chains were increased. Moreover, the obtained GPEs were thermally stable up to ~330 °C **(Figure 4**a), and two decompositions are associated with the uncomplexed (T_{d1}) and complexed (T_{d2}) polymer electrolytes. In order to clarify the plasticizing mechanism of the ILs, Wu et al. carried out a deep exploration by infrared spectroscopy characterization and density functional theory (DFT) calculations.[128] Taking the PEO-$NaClO_4$-N-methyl-N-propylpyrrolidinium bis(fluorosulfonyl)imide ($Pyr_{13}FSI$) GPE as an example, the asymmetric stretching mode of C-O-C situated at 1100 cm^{-1} was broadened and red-shifted in the presence of the IL, implying enhanced coordination with Na^+. Meanwhile, the bending mode of O=S=O underwent blue-shifting after mixing with the IL, indicating the interaction between FSI^- and PEO, which provides more Na^+ coordination sites. The charge of the O atom of PEO was reduced from -0.411 eV to -0.466 eV, and the charge of the N atom of the FSI^- anion was reduced from -0.562 eV to -0.775 eV, as calculated by DFT, which confirmed the above conclusion. Therefore, PEO was equipped with more Na^+ coordinate sites after it was plasticized, exhibiting higher solubility and lower viscosity (Figure 4b). The disadvantage, however, is that it causes a decrease in mechanical strength of the polymer electrolytes.

Several potential solid fillers, including ceramics, molecular sieves, and covalent/metal-organic frameworks, can provide space for ionic liquids penetration and preserve structural adjustment during volume expansion. Wu et al. prepared a GPE containing NaTFSI, PVDF-HFP, $Pyr_{13}FSI$, and SiO_2-based SBA-15 mesoporous molecular sieve, which showed high thermal stability and nonflammability (Figure 4c).[129] Due to the hydrogen bonding interaction between IL and SBA-15, the GPEs showed superior properties towards sodium salt dissociation, which accelerated Na^+ migration, resulting in better ionic conductivity (2.48 mS cm^{-1}) at 30 °C.

The NVP//GPE//Na showed capacity retention of 92% after 300 cycles at 30 °C.

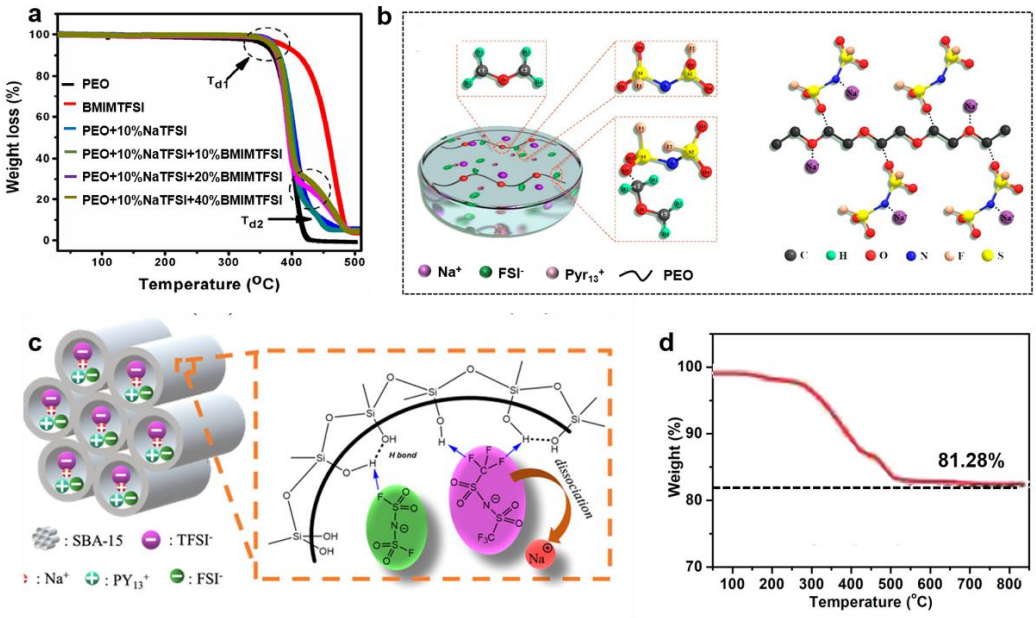

Figure 4. Principles analysis of the thermal stability of GPE containing ionic liquids. (a) Comparison of the TGA curves of different components. Reproduced with permission.[127] Copyright 2018, Springer. (b) Composition of GPE membranes and schematic illustration of FSI^- anion and PEO chain interactions. Reproduced with permission.[128] Copyright 2019, American Chemical Society. (c) Schematic diagram of the structure of Na-IL(2.3)@SBA-15, with the enlarged part showing the molecular structure and interactions between anions and SBA-15. Reproduced with permission.[129] Copyright 2020, American Chemical Society. (d) TGA curve of the NZP-PEO@IL GPE. Reproduced with permission.[130] Copyright 2022, Elsevier.

The high concentrations of ionic liquids lead to more interactions between anions and cations, thereby preventing the migration of sodium ions, resulting in an uneven distribution of ionic liquids and inhibiting the overall ion transport. For example, introducing a high content (80%) $Na_{3.4}Zr_{1.9}Zn_{0.1}Si_{2.2}P_{0.8}O_{12}$ (NZP) into a PEO-$NaClO_4$-N-propyl-N-methylpyrrolidinium bis((trifluoromethyl)sulfonyl) imide ($[Py1_3]^+[NTf_2]^-$) polymer matrix can deliver conductivity of 1.48 mS cm^{-1} at 25 °C, excellent thermal stability (81.3 wt% weight retention at 800 °C), and good interfacial stability against Na anode (Figure 4d).[130] In this system, the calculated activation energy of the GPE is 0.287 eV, which is comparable to that of the NZP (0.285 eV), demonstrating that the active NZP particles provide usable Na^+ conduction pathways. The total resistance of GPE increased and remained unchanged after 5 days due to the formation of a

kinetically stable interphase layer. Based on this GPE design, the initial discharge specific capacity of the NVP//NZP-PEO@IL//Na battery was 109.4 mAh g^{-1}, and the capacity retention was 85.4% after 150 cycles at 0.2 C.

4. GPE by *in-situ* polymerization approach

In-situ polymerization is a process in which small monomers or small solvent molecules are polymerized under the conditions of light, heat, or the presence of an initiator. It is an effective way to achieve both stable interfaces and mass production. Compared with the immersion and the solution casting approaches, the advantages of *in-situ* polymerization lie in the following points.

1) Long and short chains are cross-linked with each other to form an amorphous network structure with excellent ionic conductivity and mechanical strength.
2) The unpolymerized small molecules are confined in the cross-linked network by bonding, which improves the thermal stability and safety of the GPE.
3) In the process of *in-situ* polymerization, an interfacial layer is formed *in-situ* on the surface of the cathode and anode, which prevents the decomposition of the GPE from being catalyzed by cathode material and the formation of Na dendrites simultaneously. Meanwhile, the interface contact is also greatly improved as the *in-situ* polymerized GPE is more homogeneous.[131-135]

4.1 Separator-supported GPEs

In-situ polymerization of electrolytes on supported membranes is an effective way to obtain GPEs with high ionic conductivity, good interfacial contact, and high mechanical strength. Zhao et al. synthesized a non-flammable phosphonate-based porous cross-linked GPE through *in-situ* thermal polymerization, which had a high ionic conductivity (6.29 mS cm^{-1}) and an

electrochemical stability window that reached 4.9 V (**Figure 5**a).[136] The high ionic conductivity mainly came from the porous network structure with its ability to hold a large amount of liquid electrolyte, as well as the influence of the polar groups P=O/C=O and strong electron-withdrawing functional groups ($-CF_3$). Moreover, the polar groups P=O and C=O of monomers enhanced the solubility and compatibility of the porous network with liquid electrolytes, which are favorable for the formation of homogeneous GPEs. Based on the above design, the NVP//Na battery remained 69.17% of its initial capacity after 10000 cycles (0.64 A g^{-1}), whereas the capacity of the reference liquid electrolyte cell rapidly declined within 2500 cycles (Figure 5b).

In a different approach from the above thermal polymerization, the Ma group synthesized a GPE by ultraviolet-crosslinked boron-containing cross-linker inside a polypropylene-cellulose composite nonwoven (PCN) skeleton (B-PCPE).[137] The PCN was a mechanical reinforcing framework, and polymers with boron are anion receptors in electrolytes because of the Lewis acidity of the B element, which effectively capture the basic anions from electrolyte salts and can promote dissociation of the salts (Figure 5c). *In-situ* generation of plastic crystal polymer electrolyte took place inside the nanopores of the electrodes to facilitate ion transport in electrodes and form favorable electrode-electrolyte interfaces, providing a high-capacity retention (80.1%) after 120 cycles. Soon after, Ma et al. reported a poly(vinylene carbonate)-based composite polymer electrolyte (PVC-CPE) through dripping a mixture of vinylene carbonate (VC), tetraethylene glycol dimethyl ether (TEGDME), sodium trifluoromethanesulfonate (NaTf), and initiator into a 3D porous structured PVDF-HFP supports, followed by polymerization at 70 °C for 12 h.[138] The PVC-CPE exhibited good mechanical properties that were attributed to its 3D structure. When paired with a $NaNi_{1/3}Fe_{1/3}Mn_{1/3}O_2$ (NFM) cathode, Na^+ ions could move freely in the point contact between the active particles and the nanocracks (Figure 5d), and the full cell presented a high-capacity retention (86.8%) at 0.2 C after 250

cycles.

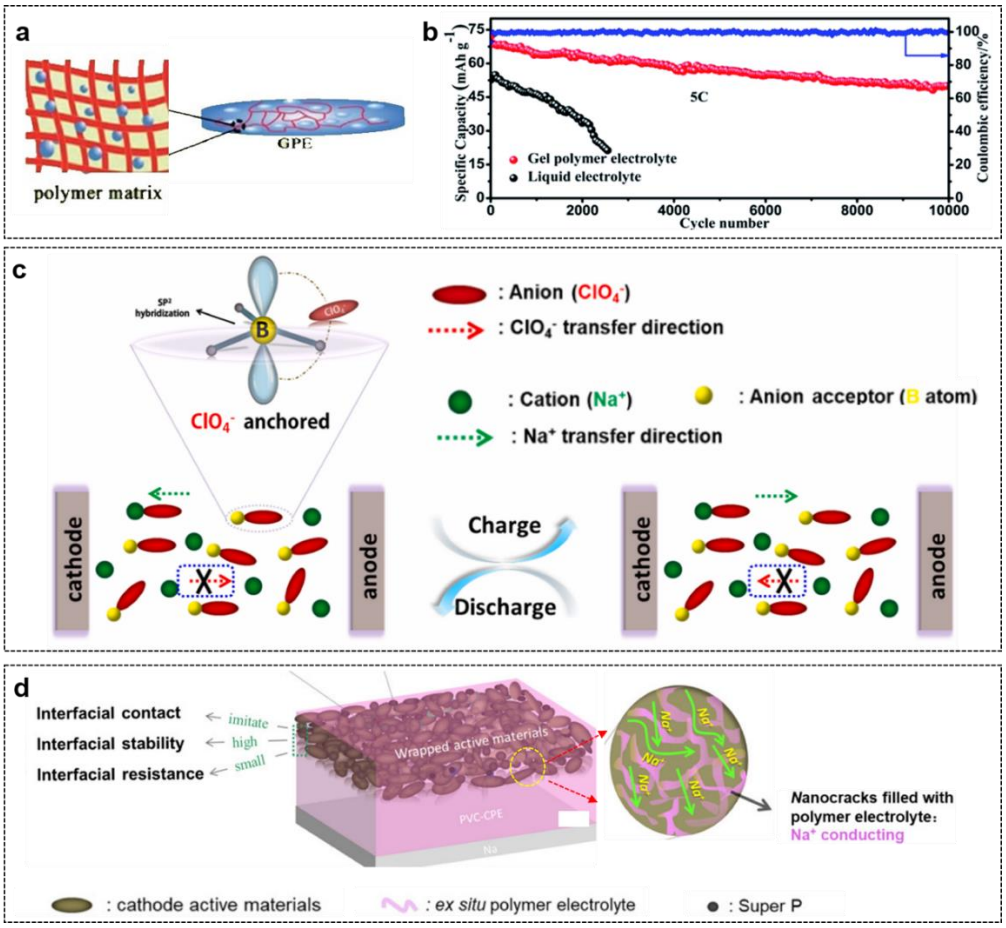

Figure 5. Properties analysis under *in-situ* polymerization approaches. (a) Schematic of the GPE structure. (b) Cycling performance of NVP//Na batteries based on GPE and liquid electrolyte. Reproduced with permission.[136] Copyright 2018, The Royal Society of Chemistry. (c) Illustration of similar single-ion transport behavior in the B-PCPE during charge-discharge processes. Reproduced with permission.[137] Copyright 2019, Elsevier. (d) Schematic of Na^+ transport and the electrode/electrolyte interface in NFM//PVC//Na cells assembled by an *in-situ* curing method. Reproduced with permission.[138] Copyright 2019, American Chemical Society.

4.2 Self-supporting GPE films

The self-supporting GPE film can form a dense and uniform solid electrolyte interfacial (SEI) film on the surface of the anode and a stable cathode electrolyte interphase (CEI) film on the cathode, which can significantly improve the interfacial impedance and electrochemical window of GPE batteries, and simultaneously improves the cycle life and energy density of the battery.[139-147] Wu et al. developed a self-supporting ethoxylated trimethylolpropane triacrylate

based quasi-solid-state electrolyte (ETPTA-$NaClO_4$-QSSE) by photopolymerization with a high ionic conductivity of 1.2 mS cm^{-1}, a wide electrochemical reaction window of >4.7 V and outstanding interfacial compatibility between the GPE and the electrode.[148] There was no obvious dendrite growth on the Na metal surface in the Na||ETPTA-$NaClO_4$-QSSE||Na battery with increasing plating time, as observed by an optical microscope, which demonstrates the outstanding interfacial stability produced by ETPTA-$NaClO_4$-QSSE. Thus, NVP||ETPTA-$NaClO_4$-QSSE||Na yielded capacity of 98 mAh g^{-1} after 1000 cycles with a high-capacity retention of 96% at a current density of 1C.

Compared with the point contact between the solid-state electrolyte and the electrode material, the precursor of the *in-situ* polymerized GPE had a viscosity similar to that of liquid electrolyte and could easily penetrate into every pore of the electrode. Then, the 3D network formed after *in-situ* polymerization provided a good path for the transport of Na^+ ions. Finally, the *in-situ* polymerized GPE could reconcile the temperature-conductivity inconsistency and form a stable electrode interfacial layer. Zhou et al. designed an *in-situ* cured GPE by introducing trihydroxymethylpropyl triacrylate (TMPTA) into conventional electrolytes, with 3D ion diffusion channels, a conformal SEI and low interface resistance (**Figure 6**a-c).[149] After X-ray photoelectron spectroscopy (XPS) analysis, it turned out that the SEI layer was rich in polyorganic and NaF content, providing a flexible layer to inhibit the interface side reactions and exhibiting a stable interface to guarantee the long-term cycling stability.

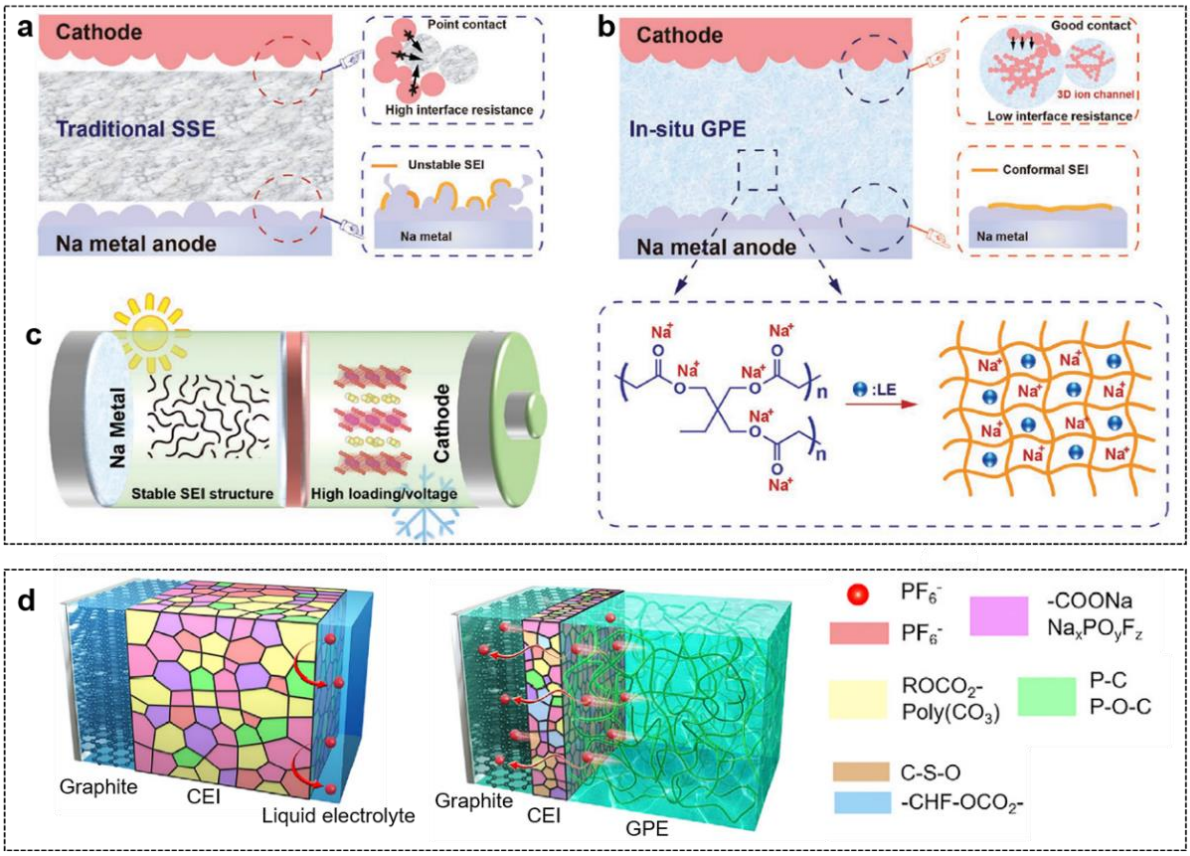

Figure 6. Interface of self-supporting *in-situ* polymerized GPE. (a) Schematic of traditional electrolyte with unstable SEI and poor interfacial contact. (b) *In-situ* polymerized GPE with a smooth SEI and good interfacial contact. (c) Illustration of the quasi-solid-state batteries. Reproduced with permission.[149] Copyright 2022, Wiley-VCH. (d) Schematic of the CEI composition on the surface of the graphite cathode in dual-ion sodium metal batteries (DISBs) using 0.5 M $NaPF_6$-PC: EMC electrolyte and GPE. Reproduced with permission.[150] Copyright 2022, Elsevier.

Meanwhile, adjusting the SEI and CEI to meet the different requirements of the electrode material for the cathode and anode interfaces is helpful to meet actual needs. Wang et al. reported a multifunctional 3D GPE obtained by *in-situ* polymerizing an ethoxylated pentaerythritol tetraacrylate (EPFA) monomer in an optimized liquid electrolyte with FEC as co-solvent and 1,3-propanesultone as additive.[150] GPEs for dual-ion sodium metal batteries (DISBs) can prevent the movement of Na^+ or PF_6^- ions towards the SEI or CEI surface defects through the interaction force from the polymer matrix. XPS measurements were performed to analyze the surface compositions of the interfacial films. The -CHF-OCO_2-substance and alkyl sulfonate

(C-S-O) in the CEI could effectively restrain the electrolyte decomposition, thus reducing the thickness of the CEI. Moreover, the F 1*s* and P 2*p* spectral peaks of PF_6^- maintained strong intensities even at a deep sputtering depth, elucidating that the uniform PF_6^- anion flux mediated by the EPTA polymeric network could successfully pass through the thin CEI and subsequently intercalate into the graphite cathode in the GPE (Figure 6d).

5. Summary and outlook

GPEs combine the high ionic conductivity and the excellent interfacial properties of organic electrolytes with the flexibility, mechanical robustness, and thermal stability of polymer electrolytes. So, GPEs are deemed more promising for practical applications than either of them. The synthesis methods for GPEs can be classified to three main types: immersion, solution casting and *in-situ* polymerization. The immersion method is simple and easy to scale up, but the obtained GPEs generally exhibit inferior thermal stability. In the case of solution-casting GPEs, the improved thermal stability is attributed to the intermolecular interactions that allow the solvent or ionic liquid to attach to the polymer substrate upon mixing. Moreover, an adjustable interfacial layer is formed *in-situ* on the surface of the cathode and anode through the *in-situ* polymerization approach, simultaneously preventing the decomposition of the GPE catalyzed by the cathode material and the formation of Na dendrites (**Figure 7**).

Despite the stupendous progress in improving the electrochemical performances of GPE Na-ion batteries, many challenges must be solved before they can be commercialized. Herein, we put forward the prospects for future development and research directions in improving the electrochemical performance of GPE Na-ion batteries:

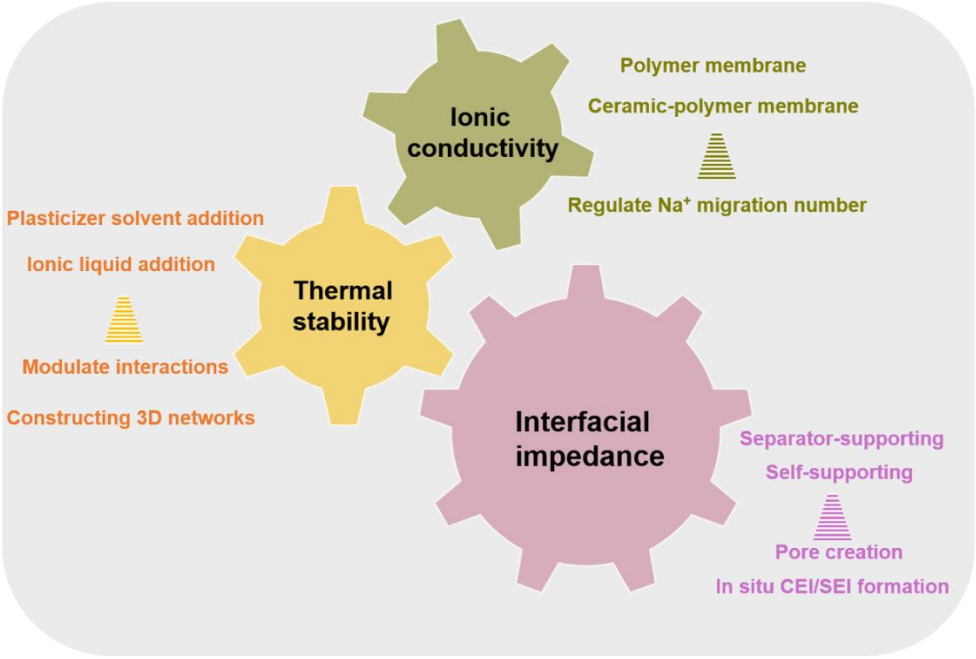

Figure 7. Summary of strategies to enhance the performance of gel polymer Na-ion batteries.

(1) Double-layer GPE design. Limited by the molecular orbital energy, a single GPE cannot meet the requirements of high oxidative ability for the cathode material and high reducibility for the anode material simultaneously. For the double-layer GPE, polymers and plasticizers with high oxidation stability can be selected for the cathode side, and polymers and plasticizers with high reduction stability can be selected for the anode side. Therefore, the obtained NIBs based on double-layer GPE may achieve much improved cycling stability during charging and discharging.

(2) *In-situ* interface layer construction. The interfacial film not only acts as a bridge between the electrode and the GPE, that is, a transport channel for sodium ions, but also a separator that hinders interfacial side reactions. The requirements of the cathode and anode for the interface film are different. The CEI film needs to be thin and dense to prevent the catalytic decomposition of the GPE by the transition metal on the cathode side. The SEI film needs to have high ionic conductivity and thermal stability to prevent interfacial side reactions on the anode side. Therefore, it is important to construct different types of interfacial layers to meet

the different requirements of the cathode and anode through additive control.

(3) Synergistic electrode protection strategies. Synergy could be achieved by considering the possible interaction between the electrode and the GPE. Specifically, through the interaction between the doping elements of the cathode material and the GPE, the decomposition of the related additives in the GPE is promoted during the charging/discharging process, and a dense CEI film is formed on the surface of the cathode. Taking $Na_{0.67}MnO_2$ cathode material as an example, this interaction may occur when iron is doped into the cathode and boron-containing salts (sodium bisoxalate borate) or small-molecule solvents (tris(trimethylsilyl) borate) are added to the GPE. In view of the chemical bonding between iron-boron, the decomposition of boron-containing molecules will be promoted during the electrochemical process, and the products are densely coated on the cathode, thereby improving the long cycle life of the battery.

(4) Combination with machine learning. Appropriate combinations of polymers, sodium salts, plasticizers and fillers can be screened through machine learning simulations. Firstly, the linear relationships between the ionic conductivity, thermal stability, interfacial properties of the GPE, and the electrochemical performance needs to be analyzed. Secondly, the relationship between the components and the electrochemical performance must be determined, as well as the decisive physical performance parameters (Lewis acidity, surface functional groups, or electronic structure). Finally, a prediction evaluation system should be simulated and established to theoretically guide the composition design of GPEs.

In conclusion, the GPE, as an important part of the battery, plays a very critical role in the performance of NIBs. Various strategies, such as electrode modification as well as interface regulation need to be combined to facilitate the practical application of GPE-based NIBs.

Conflicts of interest

There are no conflicts to declare.

Acknowledgements

H.J.F. acknowledges financial support from the Singapore Ministry of Education by Academic Research Fund Tier 2 (MOE-T2EP50121-0006).

References

[1] K. Kang, Y. S. Meng, J. Breger, C. P. Grey, G. Ceser, *Science* **2006**, *311*, 977.
[2] G. Harper, R. Sommerville, E. Kendrick, L. Driscoll, P. Slater, R. Stolkin, A. Walton, P. Christensen, O. Heidrich, S. Lambert, A. Abbott, K. Ryder, L. Gaines, P. Anserson, *Nature,* **2019**, *575*, 75.
[3] M. H. Ye, S. Z. You, J. M. Xiong, Y. Yang, Y. F. Zhang, C. C. Li, *Mater. Today Energy* **2022**, *23*, 100898.
[4] J. Pan, Y. C. Zhang, L. L. Li, Z. J. Chen, Y. L. Li, X. F. Yang, J. Yang, Y. T. Qian, *Small Methods* **2019**, *3*, 1900231.
[5] H. Y. Chen, S. L. Chen, Y. Y. Xie, H. Wang, K. Amine, X. Z. Liao, Z. F. Ma, *Energy Environ. Sci.* **2017**, *10*, 1075.
[6] Y. Li, D. X. Ye, Y. T. Sun, Y. Wang, B. Shi, W. Liu, R. Guo, H. J. Pei, H. B. Zhao, J. J. Zhang, L. Zhang, J. Y. Xie, J. L. Kong, *Mater. Today Energy* **2020**, *15*, 100368.
[7] Q. L. Ma, F. Tietz, *ChemElectroChem* **2020**, *7*, 2693.
[8] C. L. Zhao, L. L. Liu, X. G. Qi, Y. X. Li, F. X. Wu, J. M. Zhao, Y. Yu, Y. S. Hu, L. Q. Chen, *Adv. Energy Mater.* **2018**, *8*, 1703012.
[9] J. J. Kim, K. Yoon, I. Park, K. Kang, *Small Methods* **2017**, *1*, 1700219.
[10] Z. P. Li, P. Liu, K. J. Zhu, Z. Y. Zhang, Y. C. Si, Y. J. Wang, L. F. Jiao, *Energy Fuels* **2021**, *35*, 9063.
[11] C. T. Zhou, S. Bag, V. Thangadurai, *ACS Energy Lett.* **2018**, *3*, 2181.
[12] J. Y. Yang, H. H. Xu, J. Y. Wu, Z. H. Gao, F. Hu, Y. Wei, Y. Y. Liu, Z. Li, Y. H. Huang, *Small Methods* **2021**, *5*, 2100339.
[13] Y. Lu, L. Li, Q. Zhang, Z. Q. Niu, J. Chen, *Joule* **2018**, *2*, 1747.
[14] W. R. Hou, X. W. Guo, X. Y. Shen, K. Amine, H. J. Yu, J. Lu, *Nano Energy* **2018**, *52*, 279.
[15] H. L. Yang, B. W. Zhang, K. Konstantinov, Y. X. Wang, H. K. Liu, S. X. Dou, *Adv. Energy Sustainability Res.* **2021**, *2*, 2000057.
[16] S. F. Lou, F. Zhang, C. K. Fu, M. Chen, Y. L. Ma, G. P. Yin, J. J. Wang, *Adv. Mater.* **2021**, *33*, 2000721.
[17] Y. M. Wang, Z. T. Wang, F. Zheng, J. G. Sun, J. A. S. Oh, T. Wu, G. X. Chen, Q. Huang, M. Kotobuki, K. Y. Zeng, L. Lu, *Adv. Sci.* **2022**, *9*, 2105849.
[18] X. Y. Xu, Y. Y. Li, J. Cheng, G. M. Hou, X. K. Nie, Q. Ai, L. N. Dai, J. K. Feng, L. J. Ci, *J. Energy Chem.* **2020**, *41*, 73.
[19] H. B. Youcef, B. Orayech, J. M. L. D. Amo, F. Bonilla, D. Shanmukaraj, M. Armand, *Solid State Ionics* **2020**, *345*, 115168.
[20] M. D. Singh, A. Dalvi, *AIP Conf. Proc.* **2019**, *2115*, 030565.
[21] R. T. Gao, R. Tan, L. Han, Y. Zhao, Z. J. Wang, L. Y. Yang, F. Pan, *J. Mater. Chem. A* **2017**, *5*, 5273.
[22] X. M. Zhu, R. R. Zhao, W. W. Deng, X. P. Ai, H. X. Yang, Y. L. Cao, *Electrochim. Acta* **2015**, *178*, 55.

[23] C. L. Zhao, L. L. Liu, Y. X. Lu, M. Wagemaker, L. Q. Chen, Y. S. Hu, *Angew. Chem. Int. Ed.* **2019**, *58*, 17026.
[24] G. Peta, S. Bublil, H. Alon-Yehezkel, O. Breuer, Y. Elias, N. Shpigel, M. Fayena-Greenstein, D. Golodnitsky, D. Aurbach, *J. Electrochem. Soc.* **2021**, *168*, 110553.
[25] Y. J. Lim, J. Han, H. W. Kim, Y. Choi, E. Lee, Y. Kim, *J. Mater. Chem. A* **2020**, *8*, 14528.
[26] C. J. Hu, J. Z. Qi, Y. X. Zhang, S. J. Xie, B. T. Liu, G. Y. Xue, D. Q. Chen, Q. F. Zheng, P. Li, S. H. Bo, Y. B. Shen, L. W. Chen, *Nano Lett.* **2021**, *21*, 10354.
[27] J. F. Wu, Z. Y. Yu, Q. Wang, X. Guo, *Energy Storage Mater.* **2020**, *24*, 467.
[28] Y. Q. Lyu, J. Yu, J. X. Wu, M. B. Effat, F. Ciucci, *J. Power Sources.* **2019**, *416*, 21.
[29] C. X. Xing, H. T. Zhang, S. S. Pan, M. Yao, B. S. Li, Y. Q. Zhang, S. J. Zhang, *Mater. Today Energy* **2020**, *18*, 100527.
[30] W. Niu, L. Chen, Y. C. Liu, L. Z. Fan, *Chem. Eng. J.* **2020**, *384*, 123233.
[31] L. L. Liu, X. G. Qi, S. J. Yin, Q. Q. Zhang, X. Z. Liu, L. M. Suo, H. Li, L. Q. Chen, Y. S. Hu, *ACS Energy Lett.* **2019**, *4*, 1650.
[32] M. D. Singh, A. Dalvi, D. M. Phase, *Mater. Res. Bull.* **2019**, *118*, 110485.
[33] Q. Q. Zhang, Y. X. Lu, H. Yu, G. J. Yang, Q. Y. Liu, Z. X. Wang, L. Q. Chen, Y. S. Hu, *J. Electrochem. Soc.* **2020**, *167*, 070523.
[34] Y. Lu, L. Li, Q. Zhang, Y. C. Cai, Y. X. Ni, J. Chen, *Chem. Sci.* **2022**, *13*, 3416.
[35] M. Yee, K. An, D, T. Nguyen, H. W. Yun, J. Park, J. Suk, S. W. Song, *Mater. Today Energy* **2022**, *24*, 100950.
[36] E. Matios, H. Wang, J. M. Luo, Y. W. Zhang, C. L. Wang, X. Lu, X. F. Hu, Y. Xu, W. Y. Li, *J. Mater. Chem. A* **2021**, *9*, 18632.
[37] C. Devi, J. Gellanki, H. Pettersson, S. Kumar, *Sci. Rep.* **2021**, *11*, 20180.
[38] Y. W. Yao, Z. H. Liu, X. X. Wang, J. J. Chen, X. T. Wang, D. J. Wang, Z. Y. Mao, *J. Mater. Sci.* **2021**, *56*, 9951.
[39] C. Ma, K. Dai, H. S. Hou, X. B. Ji, L. B. Chen, D. G. Lvey, W. F. Wei, *Adv. Sci.* **2018**, *5*, 1700996.
[40] Q. Ma, J. J. Liu, X. G. Qi, X. H. Rong, Y. J. Shao, W. F. Feng, J. Nie, Y. S. Hu, H. Li, X. J. Huang, L. Q. Chen, Z. B. Zhou, *J. Mater. Chem. A* **2017**, *5*, 7738.
[41] X. J. Zhang, X. C. Wang, S. Liu, Z. L. Tao, J. Chen, *Nano Res.* **2018**, *11*, 6244.
[42] H. F. Fei, Y. P. Liu, C. L. Wei, Y. C. Zhang, J. K. Feng, C. Z. Chen, H. J. Yu, *Acta Phys. -Chim. Sin.* **2020**, *36*, 1905015.
[43] F. L. Xu, S. G. Deng, Q. Y. Guo, D. Zhou, Z. Y. Yao, *Small Methods* **2021**, *5*, 2100262.
[44] S. Bag, C. T. Zhou, S. Reid, S. Butler, V. Thangadurai, *J. Power Sources* **2020**, *454*, 227954.
[45] J. Pan, Y. C. Zhang, J. Wang, Z. C. Bai, R. G. Cao, N. N. Wang, S. X. Dou, F. Q. Huang, *Adv. Mater.* **2022**, *34*, 2107183.
[46] M. Vahini, M. Muthuvinayagam, *J. Mater. Sci.* **2019**, *30*, 5609.
[47] S. Wang, Q. F. Sun, Y. Ma, Z. Y. Wang, H. Z. Zhang, X. X. Shi, D. W. Song, L. Q. Zhang, L. Y. Zhu, *Small Methods* **2022**, *6*, 2200258.
[48] X. Li, S. Z. Zhang, W. Li, X. H. Xia, X. L. Wang, C. D. Gu, J. P. Tu, *Chem. Eng. J.* **2021**, *426*, 131901.
[49] A. Hamisu, S. U. Celik, *Polym. Polym. Compos.* **2019**, *27*, 149.
[50] S. Gupta, A. K. Gupta, B. K. Pandey, *Polym. Bull.* **2022**, *79*, 4999.
[51] J. Pan, H. L. Peng, Y. H. Yan, Y. Z. Bai, J. Yang, N. N. Wang, S. X. Dou, F. Q. Huang, *Energy Storage Mater.* **2021**, *43*, 165.
[52] X. G. Miao, H. Y. Wang, R. Sun, X. L. Ge, D. Y. Zhao, P. Wang, R. T. Wang, L. W. Yin, *Adv. Energy Mater.* **2021**, *11*, 2003469.
[53] S. L. Chen, F. Feng, H. Y. Che, Y. M. Yin, Z. F. Ma, *Chem. Eng. J.* **2021**, *406*, 126736.
[54] W. D. Zhou, H. C. Gao, J. B. Goodenough, *Adv. Energy Mater.* **2016**, *6*, 1501802.

[55] G. H. Chen, L. Ye, K. Zhang, M. Gao, H. Lu, H. J. Xu, Y. Bai, C. Wu, *Chem. Eng. J.* **2020**, *394*, 124885.
[56] K. Hiraoka, M. Kato, T. Kobayashi, S. Seki, *J. Phys. Chem. C* **2020**, *124*, 21948.
[57] J. Mindemark, R. Mogensen, M. J. Smith, M. M. Silva, D. Brandell, *Electrochem. Commun.* **2017**, *77*, 58.
[58] C. Sangeland, R. Younsi, J. Mindemark, D. Brandell, *Energy Storage Mater.* **2019**, *19*, 31.
[59] D. Wei, W. Shen, T. Xu, K. Li, L. Yang, Y. Zhou, M. Zhong, F. Yang, X. Xu, Y. Wang, M. Zheng, Y. Zhang, Q. Li, Z. Yong, H. Li, Q. Wang, *Mater. Today Energy* **2022**, *23*, 100889.
[60] C. S. Martinez-Cisneros, B. Pandit, C. Antonelli, J. Y. Sanchez, B. Levenfeld, A. Varez, *J. Eur. Ceram. Soc.* **2021**, *41*, 7732.
[61] J. Pan, P. Zhao, N. N. Wang, F. Q. Huang, S. X. Dou, *Energy Environ. Sci.* **2022**, *15*, 2753.
[62] P. Hu, Y. Zhang, X. W. Chi, K. K. Rao, F. Hao, H. Dong, F. M. Guo, Y. Ren, L. C. Grabow, Y. Yao, *ACS Appl. Mater. Interfaces* **2019**, *11*, 9672.
[63] M. I. Diana, P. C. Selvin, S. Selvasekarapandian, M. V. Krishna, *J. Solid State Electrochem.* **2021**, *25*, 2009.
[64] L. B. Ran, M. Li, E. Cooper, B. Luo, I. Gentle, L. Z. Wang, R. Knibbe, *Energy Storage Mater.* **2021**, *41*, 8.
[65] W. D. Zhou, Y. T. Li, S. Xin, J. B. Goodenough, *ACS Cent. Sci.* **2017**, *3*, 52.
[66] Y. W. Zheng, Q. W. Pan, M. Clites, B. W. Byles, E. Pomerantseva, C. Y. Li, *Adv. Energy Mater.* **2018**, *8*, 1801885.
[67] X. W. Yu, L. G. Xue, J. B. Goodenough, A. Manthiram, *Adv. Funct. Mater.* **2021**, *31*, 2002144.
[68] H. C. Gao, L. G. Xue, S. Xin, K. Park, J. B. Goodenough, *Angew. Chem. Int. Ed.* **2017**, *56*, 5541.
[69] L. B. Ran, S. W. Tao, I. Gentle, B. Luo, M. Li, M. Rana, L. Z. Wang, R. Knibbe, *ACS Appl. Mater. Interfaces* **2021**, *13*, 39355.
[70] S. Bublil, G. Peta, H. A-Yehezkel, Y. Elias, D. Golodnitsky, M. Fayena-Greenstein, D. Aurbach, *J. Electrochem. Soc.* **2022**, *169*, 020504.
[71] G. Y. Du, M. L. Tao, J. Li, T. T. Yang, W. Gao, J. H. Deng, Y. R. Qi, S. J. Bao, M. W. Xu, *Adv. Energy Mater.* **2020**, *10*, 1903351.
[72] Q. S. Sun, X. Chen, J. Xie, C. H. Shen, Y. Jin, C. Huang, X. W. Xu, J. Tu, B. Wang, T. J. Zhu, X. B. Zhao, J. P. Cheng, *Mater. Today Energy* **2021**, *21*, 100841.
[73] S. L. Chen, F. Feng, Y. M. Yin, H. Y. Che, X. Z. Liao, Z. F. Ma, *J. Power Sources* **2018**, *399*, 363.
[74] J. Yang, G. Z. Liu, M. Avdeev, H. L. Wan, F. D. Han, L. Shen, Z. Y. Zou, S. Q. Shi, Y. S. Hu, C. S. Wang, X. Y. Yao, *ACS Energy Lett.* **2020**, *5*, 2835.
[75] P. Jaumaux, J. R. Wu, D. Shanmukaraj, Y. Z. Wang, D. Zhou, B. Sun, F. Y. Kang, B. H. Li, M. Armand, G. X. Wang, *Adv. Funct. Mater.* **2021**, *31*, 2008644.
[76] G. Feuillade, P. Perche, *J Appl. Electrochem.* **1975**, *5*, 63.
[77] L. X. Qiao, X. Judez, T. Rojo, M. Armand, H. Zhang, *J. Electrochem. Soc.* **2020**, *167*, 070534.
[78] H. Y. Che, S. L. Chen, Y. Y.Xie, H. Wang, K. Amine, X. Z. Liao, Z. F. Ma, *Energy Environ. Sci.* **2017**, *10*, 1075.
[79] C. D. Zhao, J. Z. Guo, Z. Y. Gu, X. T. Wang, X. X. Zhao, W. H. Li, H. Y. Yu, X. L. Wu, *Nano Res.* **2022**, *15*, 925.
[80] C. M. Costa, R. Leones, M. M. Silva, S. Lanceros-Mendez, *J. Electroanal. Chem.* **2014**, *727*, 125.
[81] Y. K. Wu, W. Zhong, W. W. Tang, L. C. Zhang, H. Chen, Q. L. Li, M. W. Xu, S. J. Bao, *J. Power Sources* **2020**, *470*, 228438.
[82] M. S. Park, H. S. Woo, J. M. Heo, J. M. Kim, R. Thangavel, Y. S. Lee, D. W. Kim,

ChemSusChem **2019**, *12*, 4645.
[83] Y. D. Zhang, Y. F. An, S. Y. Dong, J. M. Jiang, H. Dou, X. G. Zhang, *J. Phys. Chem. C* **2018**, *122*, 22294.
[84] J. F. Yang, M. Zhang, Z. Chen, Z. F. Du, S. Q. Huang, B. Tang, T. T. Dong, H. Wu, Z. Yu, J. J. Zhang, G. L. Cui, *Nano Res.* **2019**, *12*, 2230.
[85] J. Z. Guo, A. B. Yang, Z. Y. Gu, X. L. Wu, W. L. Pang, Q. L. Ning, W. H. Li, J. P. Zhang, Z. M. Su, *ACS Appl. Mater. Interfaces* **2018**, *10*, 17903.
[86] P. Wang, H. R. Zhang, J. C. Chai, T. M. Liu, R. X. Hu, Z. H. Zhang, G. C. Li, G. L. Cui, *Solid State Ionics* **2019**, *337*, 140.
[87] L. Yang, Y. M. Jiang, X. M. Liang, Y. Y. Lei, T. C. Yuan, H. Y. Lu, Z. H. Liu, Y. L. Cao, J. W. Feng, *ACS Appl. Energy Mater.* **2020**, *3*, 10053.
[88] Y. Q. Yang, Z. Chang, M. X. Li, X. M. Wang, Y. P. Wu, *Solid State Ionics* **2015**, *269*, 1.
[89] J. I. Kim, Y. Choi, K. Y. Chung, J. H. Park, *Adv. Funct. Mater.* **2017**, *27*, 1701768.
[90] J. Manuel, X. H. Zhao, K. K. Cho, J. K. Kim, J. H. Ahn, *ACS Sustainable Chem. Eng.* **2018**, *6*, 8159.
[91] S. Janakiraman, O. Padmaraj, S. Ghosh, A. Venimadhav, *J. Electroanal. Chem.* **2018**, *826*, 142.
[92] M. Cheng, T. Qu, J. Zi, Y. C. Yao, F. Liang, W. H. Ma, B. Yang, Y. N. Dai, Y. Lei, *Nanotechnology* **2020**, *31*, 425401.
[93] Q. P. Yu, Q. W. Lu, X. G. Qi, S. Y. Zhao, Y. B. He, L. L. Liu, J. Li, D. Zhou, Y. S. Hu, Q. H. Yang, F. Y. Kang, B. H. Li, *Energy Storage Mater.* **2019**, *23*, 610.
[94] H. C. Gao, B. K. Guo, J. Song, K. Park, J. B. Goodenough, *Adv. Energy Mater.* **2015**, *5*, 1402235.
[95] J. I. Kim, K. Y. Chung, J. H. Park, *J. Membr. Sci.* **2018**, *566*, 122.
[96] D. H. Xie, M. Zhang, Y. Wu, L. Xiang, Y. B. Tang, *Adv. Funct. Mater.* **2020**, *30*, 1906770.
[97] P. V. K. S. Ajay, K. R. Arun, C. M. Bhaskar, M. Kamaraj, S. Ramaprabhu, *J. Electroanal. Chem.* **2020**, *859*, 113864.
[98] J. K. Kim, Y. J. Lim, H. Kim, G. B. Cho, Y. Kim, , *Energy Environ. Sci.* **2015**, *8*, 3589.
[99] X. X. Wang, Z. H. Liu, Y. H. Tang, J. J. Chen, Z. Y. Mao, D. J. Wang, *Solid State Ionics* **2021**, *359*, 115532.
[100] K. M. Freitag, P. Walke, T. Nilges, H. Kirchhain, R. J. Spranger, L. V. Wullen, *J. Power Sources* **2018**, *378*, 610.
[101] G. Piana, M. Ricciardi, F. Bella, R. Cucciniello, A. Proto, C. Gerbaldi, *Chem. Eng. J.* **2020**, *382*, 122934.
[102] R. Sathiyamoorthi, R. Chandrasekaran, S. Selladurai, T. Vasudevan, *Ionics* **2003**, *9*, 404.
[103] M. L. Lehmann, G. Yang, D. Gilmer, K. S. Han, E. C. Self, R. E. Ruther, S. R. Ge, B. R. Li, V. Murugesan, A. P. Sokolov, F. M. Delnick, J. Nanda, T. Saito, *Energy Storage Mater.* **2019**, *21*, 85.
[104] S. Parveen, P. Sehrawat, S. A. Hashmi, *ACS Appl. Energy Mater.* **2022**, *5*, 930.
[105] Y. Xue, D. J. Quesnel, *RSC Adv.* **2016**, *6*, 7504.
[106] K. Mishra, T. Arif, R. Kumar, D. Kumar, *J. Solid State Electrochem.* **2019**, *23*, 2401.
[107] W. Gao, G. Y. Du, Y. R. Qi, Q. J. Yang, W. Y. Du, M. W. Xu, *Int J Energy Res.* **2021**, *45*, 8008.
[108] C. V. S. Reddy, Q. Y. Zhu, L. Q. Mai, W. Chen, *J. Solid State Electrochem.* **2007**, *11*, 543.
[109] N. K. Jyothi, K. V. Kumar, G. S. Sundari, P. N. Murthy, *Indian J. Phys.* **2016**, *90*, 289.
[110] K. Vignarooban, P. Badami, M. A. K. L. Dissanayake, P. Ravirajan, A. M. Kannan, *Ionics* **2017**, *23*, 2817.
[111] D. Kumar, S. A. Hashmi, *J. Power Sources* **2010**, *195*, 5101.
[112] B. Jinisha, K. M. Anilkumar, M. Manoj, A. Abhilash, V. S. Pradeep, S. Jayalekshmi, *Ionics* **2018**, *24*, 1675.

[113] S. F. Song, M. Kotobuki, F. Zheng, C. H. Xu, S. V. Savilov, N. Hu, L. Lu, Y. Wang, W. D. Z. Li, *J. Mater. Chem. A* **2017**, *5*, 6424.
[114] F. Makhlooghiazad, F. Nti, J. Sun, T. C. Mendes, S. S. Malunavar, J. M. Pringle, M. Forsyth, *J. Phys. Mater.* **2021**, *4*, 034003.
[115] Y. Q. Zhao, H. Y. Wang, G. T. Gao, L. Qi, *Ionics* **2013**, *19*, 1595.
[116] S. A. Hashmi, M. Y. Bhat, M. K. Singh, N. T. K. Sundaram, B. P. C. Raghupathy, H. Tanaka, *J. Solid State Electrochem.* **2016**, *20*, 2817.
[117] M. A. A. Rani, J. Hwang, K. Matsumoto, R. Hagiwara, *J. Electrochem. Soc.* **2017**, *164*, H5031.
[118] V. K. Singh, Shalu, S. K. Chaurasia, R. K. Singh, *RSC Adv.* **2016**, *6*, 40199.
[119] S. Lee, S. J. Park, S. Kim, *Res. Chem. Intermed.* **2017**, *43*, 5403.
[120] A. Boschin, P. Johansson, *Electrochim. Acta* **2016**, *211*, 1006.
[121] D. Kumar, S. A. Hashmi, *Solid State Ionics* **2010**, *181*, 416.
[122] A. F. D. Anastro, N. Lago, C. Berlanga, M. Galceran, M. Hilder, M. Forsyth, D. Mecerreyes, *J. Membr. Sci.* **2019**, *582*, 435.
[123] D. Kumar, *Solid State Ionics* **2018**, *318*, 65.
[124] J. F. Velez, L. V. Alvarez, C. del Rio, B. Herradon, E. Mann, E. Morales, *Electrochim. Acta* **2017**, *241*, 517.
[125] M. A. Ab Rani, K. Matsumoto, R. Hagiwara, *ECS Trans.* **2016**, *75*, 431.
[126] K. Matsumoto, J. Hwang, S. Kaushik, C. Y. Chen, R. Hagiwara, *Energy Environ. Sci.* **2019**, *12*, 3247.
[127] V. K. Singh, S. K. Singh, H. Gupta, Shalu, L. Balo, A. K. Tripathi, Y. L. Verma, R. K. Singh, *J. Solid State Electrochem.* **2018**, *22*, 1909.
[128] G. H. Chen, Y. Bai, Y. S. Gao, Z. H. Wang, K. Zhang, Q. Ni, F. Wu, H. J. Xu, C. Wu, *ACS Appl. Mater. Interfaces* **2019**, *11*, 43252.
[129] Y. S. Gao, G. H. Chen, X. R. Wang, H. Y. Yang, Z. H. Wang, W. R. Lin, H. J. Xu, Y. Bai, C. Wu, *ACS Appl. Mater. Interfaces* **2020**, *12*, 22981.
[130] L. Shen, S. G. Deng, R. R. Jiang, G. Z. Liu, J. Yang, X. Y. Yao, *Energy Storage Mater.* **2022**, *46*, 175.
[131] G. H. Chen, K. Zhang, Y. R. Liu, L. Ye, Y. S. Gao, W. R. Lin, H. J. Xu, X. R. Wang, Y. Bai, C. Wu, *Chem. Eng. J.* **2020**, *401*, 126065.
[132] H. C. Gao, W. D. Zhou, K. Park, J. B. Goodenough, *Adv. Energy Mater.* **2016**, *6*, 1600467.
[133] W. Li, Z. J. Yao, S. Z. Zhang, X. L. Wang, X. H. Xia, C. D. Gu, J. P. Tu, *Chem. Eng. J.* **2021**, *423*, 130310.
[134] Q. Yi, W. Q. Zhang, S. Q. Li, X. Y. Li, C. W. Sun, *ACS Appl. Mater. Interfaces* **2018**, *10*, 35039.
[135] F. Colo, F. Bella, J. R. Nair, C. Gerbaldi, *J. Power Sources* **2017**, *365*, 293.
[136] J. Y. Zheng, Y. H. Zhao, X. M. Feng, W. H. Chen, Y. F. Zhao, *J. Mater. Chem. A* **2018**, *6*, 6559.
[137] S. L. Chen, F. Feng, Y. M. Yin, X. Z. Liao, Z. F. Ma, *Energy Storage Mater.* **2019**, *22*, 57.
[138] S. L. Chen, H. Y. Che, F. Feng, J. P. Liao, H. Wang, Y. M. Yin, Z. F. Ma, *ACS Appl. Mater. Interfaces* **2019**, *11*, 43056.
[139] C. Z. Luo, Q. Y. Li, D. Y. Shen, R. H. Zheng, D. Huang, Y. Chen, *Energy Storage Mater.* **2021**, *43*, 463.
[140] J. Y. Zheng, X. L. Liu, Y. L. Duan, L. J. Chen, X. C. Zhang, X. M. Feng, W. H. Chen, Y. F. Zhao, *J. Membr. Sci.* **2019**, *583*, 163.
[141] J. I. Kim, Y. G. Choi, Y. Ahn, D. Kim, J. H. Park, *J. Membr. Sci.* **2021**, *619*, 118771.
[142] Y. Yao, Z. Y. Wei, H. Y. Wang, H. J. Huang, Y. Jiang, X. J. Wu, X. Y. Yao, Z. S. Wu, Y. Yu, *Adv. Energy Mater.* **2020**, *10*, 1903698.

[143] F. Bella, F. Colo, J. R. Nair, C. Gerbaldi, *ChemSusChem* **2015**, *8*, 3668.
[144] X. W. Yu, L. G. Xue, J. B. Goodenough, A. Manthiram, *Adv. Energy Sustainability Res.* **2021**, *2*, 2000061.
[145] A. F. D. Anastro, L. Porcarelli, M. Hilder, C. Berlanga, M. Galceran, P. Howlett, M. Forsyth, D. Mecerreyes, *ACS Appl. Energy Mater.* **2019**, *2*, 6960.
[146] J. J. Zhang, H. J. Wen, L. P. Yue, J. C. Chai, J. Ma, P. Hu, G. L. Ding, Q. F. Wang, Z. H. Liu, G. L. Cui, L. Q. Chen, *Small* **2017**, *13*, 1601530.
[147] Y. B. Niu, Y. X. Yin, W. P. Wang, P. F. Wang, W. Ling, Y. Xiao, Y. G. Guo, *CCS Chem.* **2019**, *1*, 589.
[148] P. C. Wen, P. F. Lu, X. Y. Shi, Y. Yao, H. D. Shi, H. Q. Liu, Y. Yu, Z. S. Wu, *Adv. Energy Mater.* **2021**, *11*, 2002930.
[149] Y. N. Zhou, Z. C. Xiao, D. Z. Han, L. P. Yang, J. Y. Zhang, W. Tang, C. Y. Shu, C. X. Peng, D. Z. Zhou, *Adv. Funct. Mater.* **2022**, *32*, 2111314.
[150] X. F. Xu, K. Lin, D. Zhou, Q. Liu, X. Y. Qin, S. W. Wang, S. He, F. Y. Kang, B. H. Li, G. X. Wang, *Chem* **2020**, *6*, 902.